2017 IEEE/RSJ International Conference on Intelligent Robots and Systems (IROS)
September 24–28, 2017, Vancouver, BC, Canada

Design and Analysis of an Origami Continuum Manipulation Module with Torsional Strength

Junius Santoso, Erik H. Skorina, Ming Luo, Ruibo Yan, and Cagdas D. Onal

Abstract— **This paper presents an origami-inspired cable-driven continuum manipulator module that offers low-cost, low-volume deployment, light weight, and inherently safe human interaction and collaboration. Each module has a mass of around 110 g and integrates the actuation, sensing, and control sub-systems necessary for operation. The origami structure has 7.311 Nm/rad (0.128 Nm/degree) torsional stiffness while being capable of bending in two directions and changing arc-length down to a fully collapsed state. A maximum contraction of 35 mm and bending angle of 35.5 degrees were achieved with 45 mm arc length. The module is capable of passively supporting a 1-kg mass at its tip, or 4 additional serially connected modules, bending approximately 6 degrees in the worst case. We also show that we can actively compensate for external moments by pre-compressing or pre-bending the module. We utilize an inverse kinematic control scheme and use it for both open and closed loop control following a circular trajectory. Our results indicate that the module motion follows the desired trajectory with an RMS error of 0.681 mm in the horizontal (x-y) plane and 0.373 mm in the z-axis with closed-loop control. We also assembled two origami modules in series and drove them independently, demonstrating the proof-of-concept of a modular origami continuum manipulator.**

I. Introduction

Continuum manipulators, robot limbs inspired by trunks, snakes, and tentacles, represent a promising field in robotic manipulation research. They are well known for their compliance, as they can conform to the shape of objects they interact with. Furthermore, they also benefit from dexterity and reduced weight compared to traditional rigid manipulators. A continuum manipulator is generally composed of serially connected sections, each capable of bending in 2-D or 3-D. Such manipulators can be classified into fixed and variable length systems, of which the former type relies on a backbone while the latter is typically not backbone-supported. Variable length continuum manipulators offer greater functional range, potentially achieving fully collapsible sections. We note that compliance in the axial direction for length change also leads to weak torsional stiffness values, leading to undesired twisting deflection due to offset external forces.

Recent literature presents continuum manipulator platforms that utilize different actuation methods, including pneumatic [1], [2], hydraulic [3], and tendon-driven [4], [5], [6]. In addition, research has been done to model and simulate the behavior of a continuum manipulator. Different formulations of continuum manipulator forward kinematics exist including arc geometry, D-H parameters, Frenet-Serret frames, integral representation, and exponential coordinates as summarized in [7].

The authors are with the Mechanical Engineering Department and Robotics Engineering Program, Worcester Polytechnic Institute, MA 01609, USA. All correspondence should be addressed to Cagdas D. Onal cdonal@wpi.edu

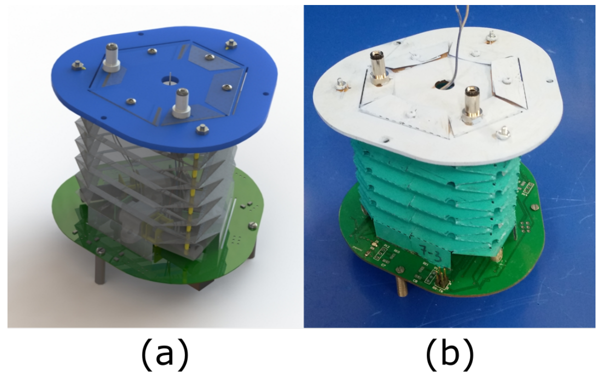

Fig. 1. (a) CAD rendering of a single origami continuum module, (b) fabricated origami continuum module.

Origami, the traditional Japanese art of folding paper, has seen growing interest from a broad range of researchers seeking to understand and utilize origami principles in technical domains [8], [9], [10]. Recently, an origami-inspired design of a foldable solar array was used to overcome the space/volume restriction associated with transporting objects to space [11]. The design allows a solar array to be folded tightly down from 25 m to 2.7 m in diameter. Origami techniques also allow for the creation of robots that are low-cost, flexible, and impact resistant [10], [12], [13].

This paper introduces a new modular cable-driven origami continuum manipulator. Each identical module of the manipulator, shown in Fig. 1, is fully integrated with three electric motors (fully-actuated), encoders, a communication bus, and a microcontroller unit (MCU) with encoder counter chips. The motors provide each module with two bending degrees-of-freedom (DoF) and a single axial DoF, allowing it to expand and retract. Each fully assembled origami module weighs about 110 g, with the motors being the heaviest part.

The origami folding pattern of the module gives it structure. A similar design in the recent literature utilizes an additional helical compression spring to maintain tension on the cables [4], [5]. In addition, Paez et al. uses an origami shell on a soft pneumatic continuum manipulator, providing protection and constraint but not serving as the main body mechanism or allowing for significant compression [14].

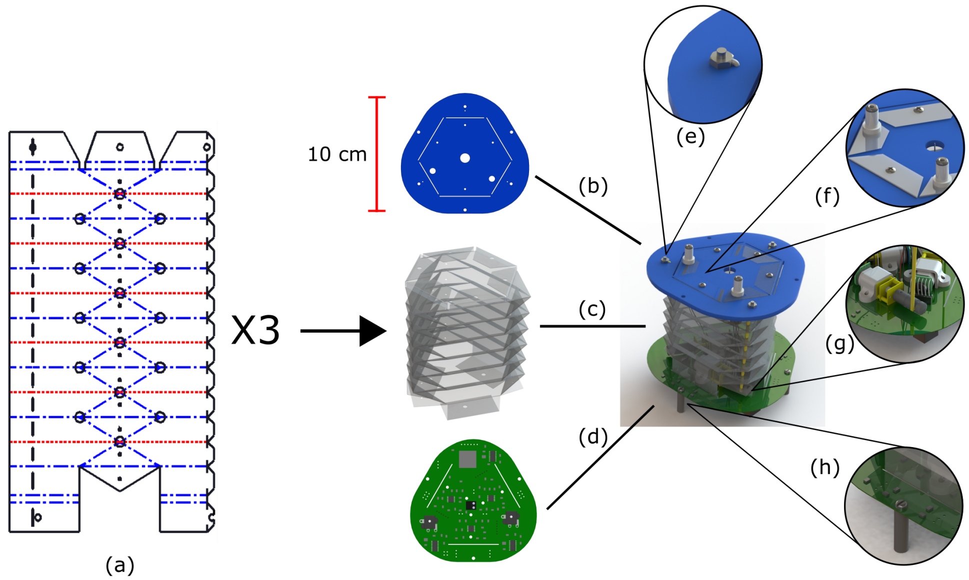

Fig. 2. (a) Yoshimura crease pattern used for the collapsible part, red dashed lines indicate the valley folds, blue dash-dot lines indicate the mountain folds and black lines indicate the cuts, three independent folded sections allows for a more uniform module, (b) acrylic top plate, (c) folded collapsible part, (d) PCB acting as bottom plate at which the motors and the collapsible part are attached to, (e) closer view of the interface between the top plate and nylon strings, strings are secured with screws and nuts, (f) two barrel jack connectors for logic and motors power to the next origami module (g) closer view of the interface between the motors and nylon strings, the yellow line indicates the nylon string, (h) 3D printed standoff to connect to the previous origami module.

Filipov et al. created modular origami structures and performed detailed analysis of their mechanical strength, but did not use them for any active mechanisms [15]. The origami mechanism employed in our work acts as a counter-spring by itself. The inherent stiffness from origami folds maintains cable tension, improves the payload capability of the modules while allowing axial compression into a fully-collapsed state, thereby reducing storage volume requirements. Applications for this manipulator include on space stations, where its light weight and minimal storage volume requirements may be useful [16].

The proposed continuum module is resistant to torsion, a characteristic that helps maintain the module shape under offset loads. When under an offset load, a continuum manipulator with low torsional stiffness would twist excessively, degrading its ability to manipulate objects. This key feature will allow for additional grasping techniques that are not normally available or favorable. For example, whole-arm grasping with a continuum arm in the horizontal plane can only be achieved with a torsionally strong design [2], [17]. To the best of our knowledge, the only related work that includes torsional stiffness analysis showed numerical results of a continuum manipulator which is almost 160 times weaker in torsion than our proposed origami module [6].

Our modular approach allows for simple control because each module can be controlled independently unlike traditional continuum manipulators, where each bending segment tends to be coupled to adjacent segments. Because the modules are independent and connected together on a communication bus, they can be scaled up to achieve functional redundancy without modification to the overall system architecture, and failed modules can be easily replaced.

In summary, the contribution of this work is the development and analysis of a new approach to continuum manipulation that:

- Uses an origami-inspired mechanism as its body, allowing for significant extension/contraction and bending motions;
- Has a high torsional strength, allowing it to resist undesired twisting deformations in 3-D space;
- Is composed of self-contained modules, whereby the addition of modules requires minimal design changes.

II. Design and Fabrication

Our proposed continuum module consists of three main parts: a foldable origami body, brushed DC micro-motors (Pololu 150:1 gear ratio and Pololu magnetic encoder with 12 counts per revolution) with pulley systems, and a controller board that offers on-board sensory measurements, feedback control, and module-to-module communication. The foldable body is constructed based on the Yoshimura crease pattern inspired by our prior work [18]. This unique structure is capable of bending in two directions and extending/retracting, while maintaining its structure and resisting torsion. Polyethylene terephthalate (PET) films were chosen as the substrate material due to their high strength to weight ratio and low cost.

The crease pattern used for this structure was designed in Solidworks and machined using an Epilog Zing laser-cutter. The pattern is shown in Fig. 2-A, where different colors indicate a variety of folds and cut. Fold lines were laser machined using a perforation pattern to reduce the stiffness so the film could be folded more easily and precisely, while preventing tears [10], [18].

The collapsible body was manually folded into 3-D following the crease pattern and later joined into an approximate triangular tube. The use of three different folded sections to create one origami module enables the module to uniformly bend in all directions. The trapezoidal sections at the right side of the crease pattern are used to lock the folded sheet, when inserted in thin slots (tab-slot lock features [19]), hence creating the hollow triangular shape shown in Fig. 2-C.

The tubular structure constructed from the crease pattern presented in this paper has a length of about 8 cm without external load. Appropriately sized-holes are cut to secure the foldable structure to the blue acrylic plate on the top and to the PCB on the bottom where the motors are secured, as shown in Fig. 2-B and 2-D. Additional holes are included for the three thin nylon cables used to drive the segment which span the length of the structure along the edges. These cables are attached to pulleys mounted on miniature motors at one end and secured with screws and nuts on the acrylic plate at the other end. Each motor is equipped with a magnetic encoder for low-level position control.

Each module is controlled by a custom printed circuit board (PCB) that uses the Atmel ATmega1280 MCU. The control board is also equipped with three DRV8801 motor drivers from Texas Instruments, capable of a peak current output of 2.8 A and three US Digital LS7366R encoder counter chips. The main task of the control board is to receive motor commands or control inputs, record the motor positions using encoders, and perform local feedback motion control. The control boards communicate using inter-intergrated circuit (I2C) protocol with different modules. An Arduino Mega 2560 board is used as an interface between the control boards and an external computer (through I2C) that handles inverse kinematics calculations for the origami module as well as data collection by an OptiTrack motion capture system.

The interface between origami modules includes two power barrel connector plugs mounted at the top (acrylic plate) of the preceding module which will connect to the female jacks soldered onto the bottom side of the PCB of the next module. In addition, the modules are secured using standoffs and screws connecting the acrylic plate of the lower module to the PCB of the upper one.

III. Kinematic Model

A. Forward Kinematics

A continuum module can be assumed to be a circular arc in 3-D space with its center in the xy plane as shown in Fig. 3. The posterior point is located at the origin while the distal point is located in 3-D space. As shown in Fig. 3-A, the homogeneous transformation from the origin frame at O to the frame attached to the tip of the segment at B can be derived as a rotation about z axis by the angle ϕ and in-plane transformation (rotation about rotated y axis (y') and translation $p = [\rho(1-\cos(\theta)), 0, \rho\sin(\theta)]^T$). If we define the curvature of the continuum module to be κ and the length of the segment to be s, then $\rho = 1/\kappa$ and $s = \theta/\kappa$. The tip position of the continuum section is then given by $[\rho\cos(\phi)(1-\cos(\theta)),\ \rho\sin(\phi)(1-\cos(\theta)),\ \rho\sin(\theta)]^T$ while the orientation is given by the product of the rotation matrix about the z and y' axes of ϕ and θ magnitudes.

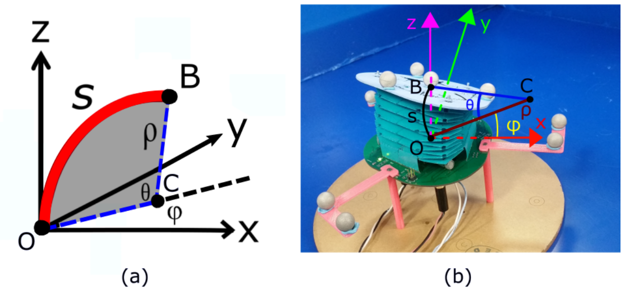

Fig. 3. (a) drawing of manipulator kinematics, (b) kinematics parameters overlaid on the physical manipulator.

In other words, each continuum segment can be fully described by three configuration parameters κ, ϕ, and s as shown in Fig. 3-B. Using the derived forward kinematics we are able to find the distal point of each continuum segment given a set of configuration parameters. This information is especially necessary when multiple origami modules are combined in series (i.e. the distal point of the previous origami module will be the posterior point of the next module). In practice, a separation due to the end connectors between modules need to be considered in multi-segment forward kinematics.

B. Inverse Kinematics

In order to control the origami module, it is necessary to develop a relationship between the configuration parameters and cable lengths. The detailed derivation for inverse kinematics of a continuum section is presented in [20]. Using the cable attachment points on the top plate of the actuator where the attachment point for cable 1 is located at 90 degrees with respect to the x axis, then the relationship between the cable lengths and the configuration parameters can be written as:

$$l_1 = 2n\sin\left(\frac{\kappa s}{2n}\right)\left(\frac{1}{\kappa} - d\sin(\phi)\right) \tag{1}$$

$$l_2 = 2n\sin\left(\frac{\kappa s}{2n}\right)\left(\frac{1}{\kappa} + d\sin\left(\frac{\pi}{3}+\phi\right)\right) \tag{2}$$

$$l_3 = 2n\sin\left(\frac{\kappa s}{2n}\right)\left(\frac{1}{\kappa} - d\cos\left(\frac{\pi}{6}+\phi\right)\right) \tag{3}$$

where l_1, l_2, and l_3 are the lengths of cables 1, 2, and 3 respectively, s, κ, ϕ are the configuration parameters as defined

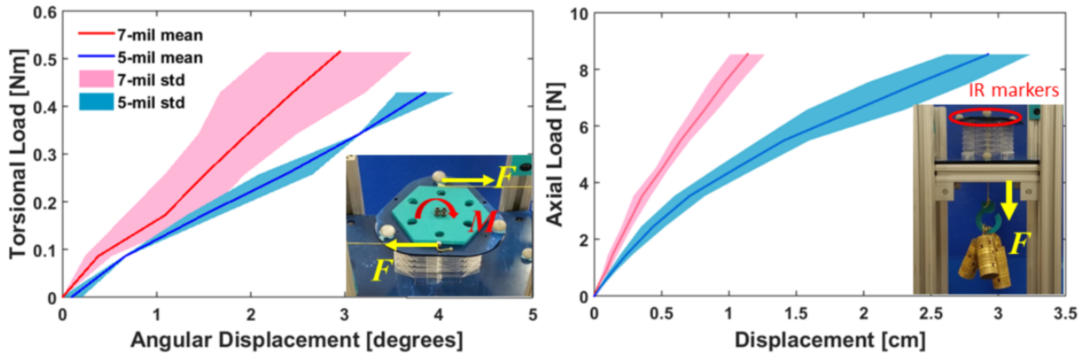

(a) (b)

Fig. 4. (a) The mean and standard deviation of torsional loading capability of the 7 and 5 mil origami modules. The data for 5 mil module was only obtained up to 0.429 Nm as the module started to twist excessively and reaching the point of failure. (b) The mean and standard deviation of torsional loading capability of the 7 and 5 mil origami modules. The modules were tested until buckling started to occur.

previously, d is the distance from the center of the mounting plate to the cable attachment point, and n is the number of sections within the larger continuum manipulator. Note that, since each origami module is operated independently, $n = 1$ for our system.

IV. Results and Discussion

A. Torsional and Axial Stiffness

In order to assess the structural properties of the proposed origami module, we conducted two experiments. The first experiment was to identify the torsional stiffness of the module, and involved loading the origami actuator with a known couple moment and measuring how much it deformed. We achieved this by fixing the actuator on one end and using suspended weights to apply equal and opposite forces on each side of the centroid, offset so as to create a pure torsional bending moment. We performed this experiment on three modules each of 0.127 mm (5 mil) and 0.178 (7 mil) thick PET with external torques up to 0.429 Nm, using an IR marker-enabled motion tracking system to record the angles.

The results are summarized in Fig. 4-A. The results show that the thicker module offers higher torsional stiffness while a thinner sheet yields a lighter structure without much decrease in torsional strength. However, the thinner material started to twist excessively at the maximum moment of 0.429 Nm, hence the experiments were not continued beyond this torque. This failure mostly happened in the regions where the origami structure was not attached to the acrylic plates. The actuators constructed with thicker PET films did not show signs of failure up to 0.515 Nm, a relatively large torque compared with the weight of the origami film. The average torsional stiffness for 7 mil and 5 mil modules are 0.128 Nm/deg and 0.110 Nm/deg, respectively.

Axial loading experiments were conducted by keeping the modules upright clamping the bottom end-plate and using known payloads up to 0.87 kg for both 7 mil and 5 mil film. The known payload was attached to the top acrylic plate of the actuator hence compressing the origami structure. In this experiment, the load was increased until the actuator started to buckle. In contrast to the torsional stiffness profile, Fig. 4-B reveals that the axial stiffness varies more significantly with changing film thickness. This was expected because origami folds act like springs, whereby thinner substrates offer lower stiffness. Moreover, the 5 mil modules exhibit more nonlinear behavior compared to the 7 mil ones. By calculating the slope of the graph we can determine an average spring constant of the origami body in the axial direction. This translates to the payload capability of the modules without additional springs. The average spring constants were found to be 7.482 N/cm and 2.877 N/cm for film thicknesses of 7 mil and 5 mil, respectively. From these initial findings, 7 mil modules offer better performance to be used in a continuum manipulator, where its higher torsional and axial stiffness allows the module to better withstand external forces. A full list of module parameters can be found in Table I.

TABLE I
Module Parameters

Mass	110 g
Origami Structure Radius	3.5 cm
Uncompressed	6.5 cm
Fully Compressed Length	3.0 cm
Axial Stiffness	7.482 N/cm
Torsional Stiffness	7.311 Nm/rad

B. Bending Stiffness

We investigated the bending stiffness of our module by applying loads in a horizontal cantilever configuration. The orientation of the acrylic plate at the free end with respect to the vertical plane is defined as the bending angle and measured using an IR motion tracking system. First, we investi-

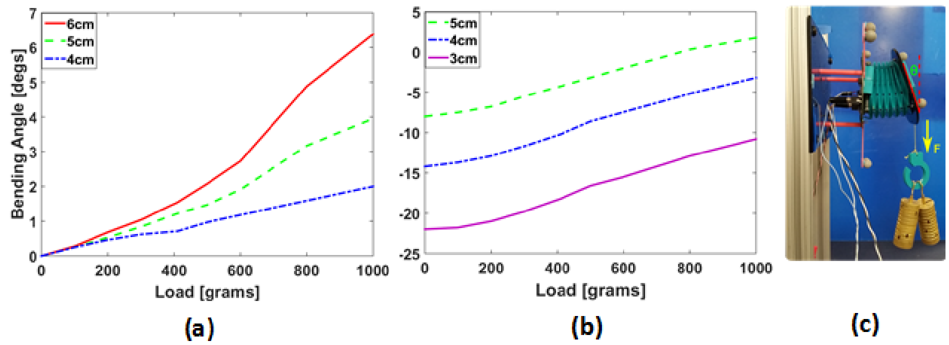

Fig. 5. (a) Result for an origami module with 3 actuated motors forming a straight continuum section, (b) with only 1 (top) motor actuated forming a curved section, (c) experimental setup where the origami module is loaded in a cantilever configuration.

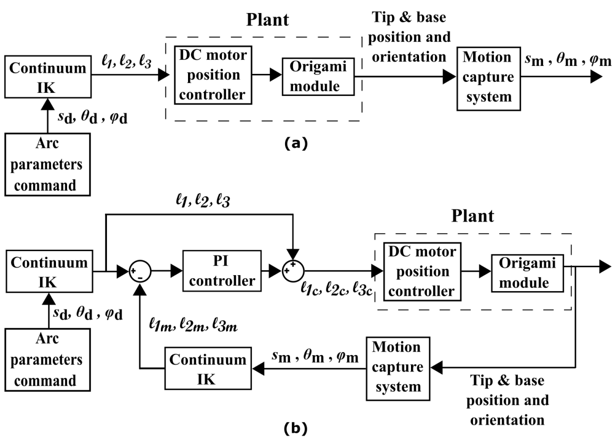

Fig. 6. Control architecture for: a) open-loop, (b) closed-loop.

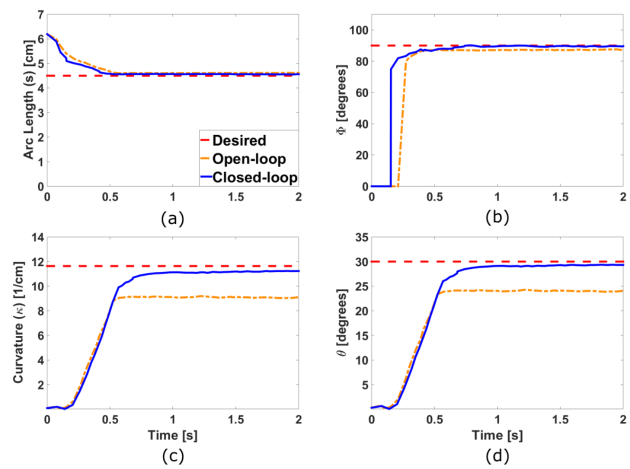

Fig. 7. Step response of a single module given a configuration s = 4.5 cm, ϕ = 90 degrees, κ = 11.64, and θ = 30 degrees. Results shown for both open and closed-loop control.

gated the module behavior without compensation, where we fixed each cable at a constant length and applied payloads. It should be noted that due to the lack of backdrivability in the motors, this is similar to an entirely passive response. We tested this for three separate actuation lengths, results of this experiment can be seen in Fig. 5-A. We found that when fully extended, the module will bend by 6.38 degrees under a load of 1 kg. This configuration represents a worst-case scenario, with a fully extended, passive actuator. This load is equivalent to about 4 additional modules mounted serially.

We also investigated the ability of the manipulator to compensate for these loads by actuating in opposition to the force as shown in Fig. 5-C. We actuated a single cable to a specific length, which bent the actuator in the opposite (negative) direction, and repeated the same bending experiment, the results of which are shown in Fig. 5-B. This allows the actuator to stay level under greater forces, but with the trade-off of losing some control on the module shape or range of controllable motion. Fully actuated, a single module can hold around 6 serially mounted modules horizontally before deforming more than 5 degrees, giving us an idea of how long a chain of modules could be before design changes may be necessary.

C. System Response

To evaluate the performance of the proposed origami module, we conducted step response experiments with both open and closed-loop control shown in Fig. 6. The experiments commanded the actuator to reach a certain configuration parameter set: arc length (s), θ, and ϕ, as described in the kinematic modeling section, using a low-level PID controller on the motor encoder position.

To evaluate the performance of the origami continuum manipulator module in terms of its capability to reach a desired set of configuration parameters, we performed experiments in a custom motion capture environment, comprising four OptiTrack IR cameras. These cameras track passive IR markers attached to the top and bottom end connectors of the module to experimentally measure the configuration of the origami continuum module. The measurements were transferred to a desktop computer through an ethernet connection for processing.

The configuration parameters were found from the centroid and orientation of the bottom and top plates of the

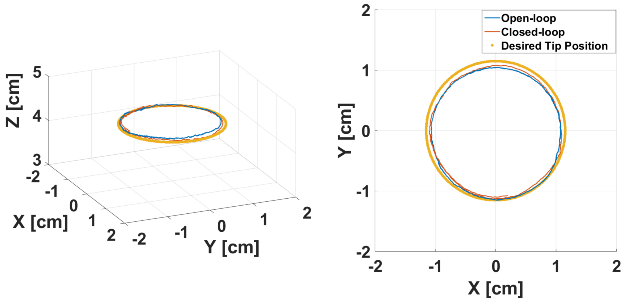

Fig. 8. Circular tracking with the proposed origami continuum module using open and closed-loop control.

module. Assuming that the origami module only experiences bending in a plane, angle θ is equal to the dot product between the frames attached to the bottom and top plates. Once θ is determined, we calculate the value of ρ using the cosine rule, and curvature κ is defined as $1/\rho$. Lastly, the bending plane angle ϕ is determined using trigonometry. Since the motion capture system is capable of tracking the position of the markers with sub-millimeter resolution, even a slight difference in tip and base positions will result in a non-zero ϕ reading. Thus, we implemented a simple filter that utilizes a small dead-zone ϵ around zero.

The open-loop control of the origami actuator is based on the inverse kinematics of a continuum section (1), (2), (3), which we used to find the required cable lengths (l_1, l_2, l_3), that will shape the module into the desired configuration (s_d, θ_d, ϕ_d), as shown in Fig. 6. The cable lengths are converted into encoder positions, which are then sent to the low-level controller as reference signals.

The closed-loop control takes into account the difference between the desired cable lengths generated from the inverse kinematics (l_1, l_2, l_3) and the cable lengths obtained through a conversion of the measured configuration parameters (l_{1m}, l_{2m}, l_{3m}). A PI controller that regulates the errors between the desired and measured cable lengths is added to the open-loop feedforward commands, producing final motor commands (l_{1c}, l_{2c}, l_{3c}).

Fig. 7 shows the results of step response for both open and closed-loop control, at which the configuration parameters were tracked. The results show that the closed-loop control is able to bring the system to reach the desired configuration. No overshoot is observed and the rise times are 0.5 s for both control schemes. These results also imply that the inverse kinematics model was successful in bringing the actuator close to the desired configuration.

D. Circle Tracking

The dynamic response of the proposed module was evaluated by performing a circle tracking experiment. A circular trajectory was generated varying the ϕ values over the range of [0, 2π] while keeping the desired arc length and curvature constant. For this experiment we kept the same values of arc length and curvature as the ones used in the step response experiment in Fig. 7. The tip position of the actuator was tracked using motion capture as explained earlier and compared to the desired trajectory. Fig. 8 displays the results of this experiment with the desired and tracked tip trajectories in 3-D (left) and in 2-D (right), with quantitative results summarized in Table II.

TABLE II

CIRCLE TRACKING RESULTS

	Open Loop	Closed Loop
Max Horizontal Error	1.237 mm	1.097 mm
RMS Horizontal Error	0.734 mm	0.681 mm
Max Vertical Error	0.970 mm	0.820 mm
RMS Vertical Error	0.579 mm	0.373 mm

These results indicate that our system is well-calibrated and open-loop control may provide successful tracking of desired paths under no disturbances, but feedback will likely be required to compensate for modeling errors and disturbances during system operation. Moreover, the larger error difference observed on the step response (especially on κ and θ) compared to the error for the circle follow experiment also suggest that the system can still reliably reach the desired task-space goal despite a relatively large error on the configuration space.

E. Multi-module Motion Evaluation

As a proof-of-concept case study, two origami modules were connected in series, as shown in Fig. 9. This figure displays snapshots of the combined two-module system following a circular tip trajectory while keeping the top plate parallel to ground, allowing for an object to be placed on top and kept from falling. This maneuver was achieved by keeping the arc length and θ for both modules to be the same and sweeping the ϕ values over the range of [0, 2π] with an offset of π. Independent control of each origami module was demonstrated without any modification of the system architecture.

V. CONCLUSION AND FUTURE WORK

This paper focused on a novel approach for an origami-inspired modular continuum manipulator with torsional strength. Origami modules were designed and analyzed for their axial, torsional, and bending deformations. Both open and closed-loop step responses of the proposed continuum modules were investigated. When exposed to a step input, the origami module is able to go to the desired configuration and reach a steady state within 1 s. A circle following routine was tested on a single module, and the results show that the actuator is capable of following the commanded trajectory within reasonable error bounds. No significant improvement was observed when a closed-loop control scheme was introduced to the system because the feed-forward term generated from the inverse kinematics of a continuum section was able to bring the actuator close to the desired configuration parameters. However, further testing involving

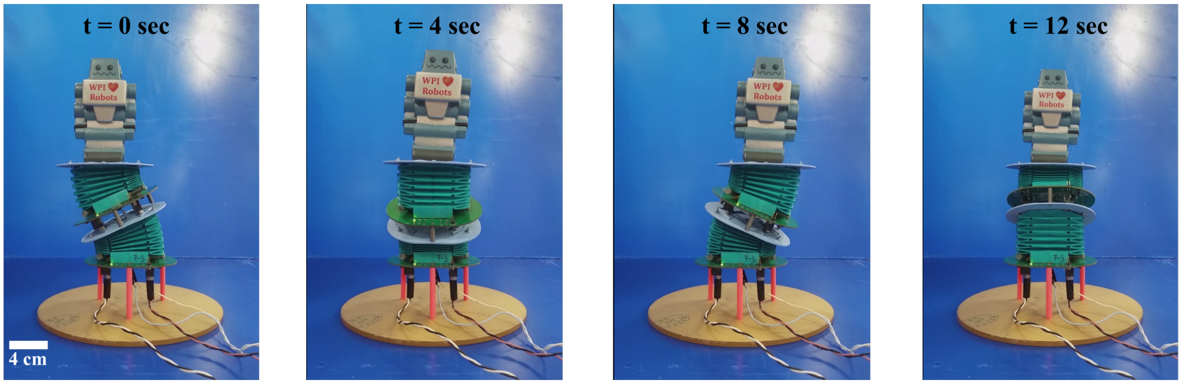

Fig. 9. Two combined actuators executing circle follow trajectory while keeping the top plate parallel to the ground, a small doll was placed on top of the plate and was able to stay balanced.

external disturbances and faster tracking velocities will be appropriate to test the response of the closed-loop control.

Preliminary analysis on inherent problems in designing modular robots was considered [21], which will be extended in future work for multi-modular arms. Other future work includes incorporating proprioceptive sensors onto the modules to eliminate the use of a motion capture system and in-depth analysis on the multi-module origami manipulator dynamics and control. In addition, more advanced control schemes will be evaluated to explore more realistic dynamic tracking scenarios with a multi-segmented origami continuum arm. Finally, we would like to further investigate possible applications, including to assist astronauts on space missions.

ACKNOWLEDGMENT

We would like to thank Shadi T. Kalat for her help with the motion capture system and Julia Szemiot for her thoughtful comments on this manuscript.

REFERENCES

[1] G. Gerboni, T. Ranzani, A. Diodato, G. Ciuti, M. Cianchetti, and A. Menciassi, "Modular soft mechatronic manipulator for minimally invasive surgery (mis): overall architecture and development of a fully integrated soft module," *Meccanica*, vol. 50, no. 11, pp. 2865–2878, 2015.

[2] W. McMahan, B. A. Jones, and I. D. Walker, "Design and implementation of a multi-section continuum robot: Air-octor," in *2005 IEEE/RSJ International Conference on Intelligent Robots and Systems*, pp. 2578–2585, IEEE, 2005.

[3] Y. Bailly and Y. Amirat, "Modeling and control of a hybrid continuum active catheter for aortic aneurysm treatment," in *Proceedings of the 2005 IEEE International Conference on Robotics and Automation*, pp. 924–929, IEEE, 2005.

[4] D. J. Zhang K, Qiu C, "An extensible continuum robot with integrated origami parallel modules," *Journal of Mechanisms and Robotics*, vol. 8, no. 3, p. 0310010, 2016.

[5] M. Salerno, K. Zhang, A. Menciassi, and J. S. Dai, "A novel 4-dof origami grasper with an sma-actuation system for minimally invasive surgery," *IEEE Transactions on Robotics*, vol. 32, pp. 484–498, June 2016.

[6] P. Qi, C. Qiu, H. Liu, J. S. Dai, L. D. Seneviratne, and K. Althoefer, "A novel continuum manipulator design using serially connected double-layer planar springs," *IEEE/ASME Transactions on Mechatronics*, vol. 21, pp. 1281–1292, June 2016.

[7] R. J. Webster and B. A. Jones, "Design and kinematic modeling of constant curvature continuum robots: A review," *The International Journal of Robotics Research*, 2010.

[8] R. J. Lang, "A computational algorithm for origami design," in *Proceedings of the twelfth annual symposium on Computational geometry*, pp. 98–105, ACM, 1996.

[9] B. Saccà and C. M. Niemeyer, "Dna origami: the art of folding dna," *Angewandte Chemie International Edition*, vol. 51, no. 1, pp. 58–66, 2012.

[10] C. D. Onal, M. T. Tolley, R. J. Wood, and D. Rus, "Origami-inspired printed robots," *IEEE/ASME Transactions on Mechatronics*, vol. 20, pp. 2214–2221, Oct 2015.

[11] S. A. Zirbel, M. E. Wilson, S. P. Magleby, and L. L. Howell, "An origami-inspired self-deployable array," in *ASME 2013 Conference on Smart Materials, Adaptive Structures and Intelligent Systems*, pp. V001T01A026–V001T01A026, American Society of Mechanical Engineers, 2013.

[12] K. Jayaram and R. J. Full, "Cockroaches traverse crevices, crawl rapidly in confined spaces, and inspire a soft, legged robot," *Proceedings of the National Academy of Sciences*, vol. 113, no. 8, pp. E950–E957, 2016.

[13] S. M. Felton, M. T. Tolley, C. D. Onal, D. Rus, and R. J. Wood, "Robot self-assembly by folding: A printed inchworm robot," in *Robotics and Automation (ICRA), 2013 IEEE International Conference on*, pp. 277–282, IEEE, 2013.

[14] L. Paez, G. Agarwal, and J. Piak, "Design and analysis of a soft pneumatic actuator with origami shell reinforcement," *Soft Robotics*, vol. 3, no. 3, p. 11, 2016.

[15] E. T. Filipov, T. Tachi, and G. H. Paulino, "Origami tubes assembled into stiff, yet reconfigurable structures and metamaterials," in *Proceedings of the National Academy of Sciences of the United States of America*, vol. 112, p. 1232112326, 2015.

[16] B. Dunbar, "Advanced space transportation program: Paving the highway to space," April 2008.

[17] W. McMahan, V. Chitrakaran, M. Csencsits, D. Dawson, I. D. Walker, B. A. Jones, M. Pritts, D. Dienno, M. Grissom, and C. D. Rahn, "Field trials and testing of the octarm continuum manipulator," in *Proceedings 2006 IEEE International Conference on Robotics and Automation, 2006. ICRA 2006.*, pp. 2336–2341, May 2006.

[18] C. D. Onal, R. J. Wood, and D. Rus, "An origami-inspired approach to worm robots," *IEEE/ASME Transactions on Mechatronics*, vol. 18, no. 2, pp. 430–438, 2013.

[19] S. G. Faal, F. Chen, W. Tao, M. Agheli, S. Tasdighikalat, and C. D. Onal, "Hierarchical kinematic design of foldable hexapedal locomotion platforms," *JMR*, vol. 3, no. 4L3, p. 1, 2015.

[20] B. A. Jones and I. D. Walker, "Kinematics for multisection continuum robots," *IEEE Transactions on Robotics*, vol. 22, no. 1, pp. 43–55, 2006.

[21] C. Wright, A. Buchan, B. Brown, J. Geist, M. Schwerin, D. Rollinson, M. Tesch, and H. Choset, "Design and architecture of the unified modular snake robot," in *Robotics and Automation (ICRA), 2012 IEEE International Conference on*, pp. 4347–4354, IEEE, 2012.